

iDADwgl - a R package for open-system uranium-thorium dating

Anthony Dosseto^{1,} and Ben Marwick²*

2018-12-21

¹Wollongong Isotope Geochronology Laboratory, School of Earth & Environmental Sciences. University of Wollongong. Wollongong NSW Australia

²Department of Anthropology, University of Washington, Seattle, WA, USA

*Corresponding author: tonyd@uow.edu.au

Introduction

Open-system uranium-thorium (U-Th) dating of teeth and bones, while challenging, has revolutionised our ability to provide reliable chronology for humans and fauna (Eggins et al., 2005; Sambridge et al., 2012; Grün et al., 2014). Thus, this approach has significantly improved our understanding of human evolution (e.g. Dirks et al., 2017; Sutikna et al., 2016). Uranium-thorium dating is based on the premise that a material takes up U but no Th, so all the ^{230}Th in the sample comes from decay of ^{238}U . If detrital Th is included to the sample, a correction must be included to account for the fraction of ^{230}Th which is detrital and not derived from ^{238}U decay. Another requirement is that there is no gain or loss of ^{230}Th , ^{234}U or ^{238}U after formation of the material. While it is often the case for many geological samples such as corals or speleothems, this requirement is rarely met for teeth and bone (although enamel can sometimes be quite impervious to isotope gain or loss). Thus, for teeth and bone, U-Th dating requires to take into account open system behaviour. The diffusion-adsorption-decay (DAD) model developed by Sambridge et al. (2012) was instrumental to implement successfully open-system U-Th dating. It allows for advective and diffusive transport of uranium and thorium isotopes, while include synchronous radioactive decay. The software implementation was written in Fortran and is available as a Java GUI (<http://www.earth.org.au/codes/iDaD/>). In this article, we propose a R package which implements the model of Sambridge et al. (2012).

The motivation for providing this model as an R package is to increase the transparency, reproducibility, and flexibility of the analytical workflow for computing U-Th ages. Currently it is difficult to include the Java GUI in a fully scripted data analysis so the method for computing the DAD model is not highly transparent. This can obscure steps where key decisions are made that are important for others to see to verify the reliability of the analysis. Enabling a scripted workflow for computational analysis of geoscience data is important for improving the reproducibility of results. Reproducibility refers the ability to recreate the results or retest the hypotheses leading to a scientific claim, either by rerunning the same code used by the original authors, or by writing new code. High rates of irreproducibility of research results have been estimated in several fields and disciplines (Ioannidis, 2005; Institute, 2013; Collaboration and others, 2015; Freedman et al., 2015; Medical Sciences, 2015; Camerer et al., 2016; Camerer et al., 2018). Consequently, the transparency, openness, and reproducibility of results and methods are receiving increased attention, and the norms of research in many fields are changing (Miguel et al., 2014; Nosek et al., 2015).

There is strong interest in open, transparent, and reusable research in the geoscience community (Gil et al., 2016) and substantial progress toward open data has been made in the geosciences with the widespread use of data services of NASA, USGS, NOAA and community-built data portals such as OneGeology, EarthChem, RRUFF, PANGAEA, PaleoBioDB, and others (Kattge et al., 2014; Ma, 2018). However, the use of open source software such as R (Pebesma et al., 2012), and sharing of scripted data analysis workflows with research publications is not yet widespread (Hutton et al., 2016). With this R package our goal is to make

scripted and reproducible data analysis easy for open-system uranium-thorium dating. This will improve the transparency of geochronology research, and provide a more credible and robust foundation for scientific advancement (Hutton et al., 2016).

Methods

Data required for the DAD model are ($^{230}\text{Th}/^{238}\text{U}$) and ($^{234}\text{U}/^{238}\text{U}$) activity ratios collected along a transect perpendicular to the surface of the tooth or bone (brackets denote activity ratios throughout this article). Sampling for analysis can be done by micro-drilling or laser ablation. If the former, aliquots are then dissolved, followed by separation of U and Th using ion exchange chromatography. This is more time consuming (at least one week of work) than laser ablation, where the material sampled by the laser is directly sent to the mass spectrometer.

While laser ablation also offers a better spatial resolution than micro-drilling, the precision of the data is inferior because of the much smaller amount of material sampled. Uranium and thorium isotope ratios are then analysed by multi-collector inductively-coupled plasma mass spectrometry. A plasma ionise all U and Th atoms, their isotopes are separated through a magnetic field and each collected in a different collector. If using laser ablation, it is best to have two ion counters so ^{230}Th and ^{234}U can be collected simultaneously.

The distance of each analysis location from the inner and outer surfaces of the bones, for instance, needs to be recorded. One surface is given a coordinate of 1 and the other one -1, thus coordinates of analyses take values in between (Figure 1).

Installing and attaching the package

To run the model, start R and install the package from GitHub. There are many ways to do this, one simple method is shown in the line below. This only needs to be done once per computer.

```
source("https://install-github.me/tonydoss/iDADwig1")
```

For routine data analysis, R scripts need to contain this line to attach the package to the current working environment. This line needs to be run at the start of each analysis:

```
# attach the package  
library(iDADwig1)
```

Input data format

The key function of our package, `iDADwig1()` requires a data frame with the following column names:

- `iDAD.position`
- `U234_U238_CORR`
- `U234_U238_CORR_Int2SE`
- `iDAD.position.1`
- `Th230_U238_CORR`
- `Th230_U238_CORR_Int2SE`
- `U_ppm`
- `U_ppm_Int2SE`

This data frame can be created by importing an Excel or CSV file into the R environment using a generic function such as `read.csv` or `read_excel` from the `readxl` package (Wickham and Bryan, 2018). To help with preparing data for input into our function, we have included two examples of input files. The code chunk below shows how to access one of the two example CSV files included in the package, and how to read it into the R environment.

```
# get the path the one of the CSV files included in the package
path_to_included_example_csv_file <-
  system.file("extdata",
              "input/Hobbit_MH2T_for_iDAD.csv",
              package = "iDADwig1",
              mustWork = TRUE)

# read in the example CSV file included in the package
Hobbit_MH2T_for_iDAD <-
  read.csv(path_to_included_example_csv_file)
```

73 Table 1 shows the data contained in the `Hobbit_MH2T_for_iDAD.csv` file included in the package

Table 1 Data contained in the example CSV file `Hobbit_MH2T_for_iDAD.csv` included in the package

| iDAD.position | U234_U238_CORR | U234_U238_CORR_Int2SE | iDAD.position.1 | Th230_U238_CORR | Th230_U238_CORR_Int2SE | U_ppm | U_ppm_Int2SE |
|---------------|----------------|-----------------------|-----------------|-----------------|------------------------|-------|--------------|
| -0.9558824 | 1.2696216 | 0.00421 | -0.9558824 | 0.0733000 | 0.00226 | 12.3 | 0.615 |
| -0.8568112 | 1.2729341 | 0.00424 | -0.8568112 | 0.0732000 | 0.00238 | 12.7 | 0.635 |
| -0.7577400 | 1.2654235 | 0.00372 | -0.7577400 | 0.0760000 | 0.00177 | 12.5 | 0.625 |
| -0.6586688 | 1.2673451 | 0.00454 | -0.6586688 | 0.0770000 | 0.00193 | 14.2 | 0.710 |
| -0.5595975 | 1.2691554 | 0.00291 | -0.5595975 | 0.0721000 | 0.00188 | 19.8 | 0.990 |
| -0.4605263 | 1.2655151 | 0.00284 | -0.4605263 | 0.0769000 | 0.00167 | 18.0 | 0.900 |
| -0.3614551 | 1.2669790 | 0.00255 | -0.3614551 | 0.0816000 | 0.00169 | 20.0 | 1.000 |
| -0.2623839 | 1.2760185 | 0.00231 | -0.2623839 | 0.0786000 | 0.00126 | 27.2 | 1.360 |
| -0.1633127 | 1.2655140 | 0.00228 | -0.1633127 | 0.0753000 | 0.00124 | 26.7 | 1.335 |
| -0.0642000 | 1.2766815 | 0.00210 | -0.0642000 | 0.0731000 | 0.00098 | 0.3 | 0.015 |
| 0.0348000 | 1.2706338 | 0.00223 | 0.0348000 | 0.0779000 | 0.00152 | 33.9 | 1.695 |
| 0.1339009 | 1.2642664 | 0.00242 | 0.1339009 | 0.0666000 | 0.00138 | 37.7 | 1.885 |
| 0.2329721 | 1.2662201 | 0.00273 | 0.2329721 | 0.0713000 | 0.00138 | 30.7 | 1.535 |
| 0.3320434 | 1.2649714 | 0.00224 | 0.3320434 | 0.0773000 | 0.00185 | 25.2 | 1.260 |
| 0.4311145 | 1.2655783 | 0.00284 | 0.4311145 | 0.0832000 | 0.00147 | 28.9 | 1.445 |
| 0.5301858 | 1.2679863 | 0.00264 | 0.5301858 | 0.0864000 | 0.00162 | 29.0 | 1.450 |
| 0.6292570 | 1.2644629 | 0.00258 | 0.6292570 | 0.0816000 | 0.00162 | 27.5 | 1.375 |
| 0.7283282 | 1.2627009 | 0.00200 | 0.7283282 | 0.0704000 | 0.00132 | 30.1 | 1.505 |
| 0.8273994 | 1.2658484 | 0.00471 | 0.8273994 | 0.0953000 | 0.00175 | 19.6 | 0.980 |
| 0.9264706 | 1.2626681 | 0.00316 | 0.9264706 | 0.0958000 | 0.00232 | 14.8 | 0.740 |

74 The columns `iDAD.position`, `U234_U238_CORR`, `U234_U238_CORR_Int2SE`, `Th230_U238_CORR` and
75 `Th230_U238_CORR_Int2SE` must be present in the input data frame with these exact names for the
76 model to function. The `iDADwig1()` function will check if the input data frame has these columns, and will
77 stop with an error message if it does not find these columns. The `names` function can be used to update
78 column names of a data frame to ensure they match the names that the model function requires. The order
79 of the columns in the data frame is not important.

80 The `iDAD.position` column corresponds to the coordinates of the ($^{234}\text{U}/^{238}\text{U}$) analyses, which as indicated
81 above take values between -1 and 1 (Figure 1). The second `iDAD.position.1` column is used if the coordi-
82 nates of the ($^{230}\text{Th}/^{238}\text{U}$) analyses are different from those of the ($^{234}\text{U}/^{238}\text{U}$) analyses.

83 Columns `U234_U238_CORR` and `U234_U238_CORR_Int2SE` are the ($^{234}\text{U}/^{238}\text{U}$) activity ratios and their 2σ

84 errors. Columns Th230_U238_CORR and Th230_U238_CORR_Int2SE are the ($^{230}\text{Th}/^{238}\text{U}$) activity ratios and
85 their 2σ errors.

86 Columns U_ppm and U_ppm_Int2SE and calculated uranium concentrations (in ppm) and their 2σ errors.
87 Uranium concentrations are not necessary for the model and only used for display of the U concentration
88 profile in a figure.



Figure 1. Modern human femur (132A/LB/27D/03) from Liang Bua, Flores, Indonesia. Two analysis transects can be seen. For a given transect, the outer and inner surface of the bone are given 1 and -1 reference coordinates, and the position of each analysis is calculated accordingly. Modified from Sutikna et al. (2016).

Details of the input parameters

Our key function, `iDADwig1()` has several arguments that need to be set before we can get meaningful results.

`nbit` is the number of iterations. For the first run, set to 1.

`fsum_target` is the sum of the squared differences between the calculated and observed activity ratios. Give it a low value to start with (e.g. 0.05). If script takes too long, try a higher value for `fsum_target`.

`U48_0_min` and `U48_0_max` are the minimum and maximum values allowed for the ($^{234}\text{U}/^{238}\text{U}$) activity ratio at the surface of the sample. Since ($^{234}\text{U}/^{238}\text{U}$) does not vary greatly over the time period generally studied, the values measured near the surface of the sample can be used as a guide. These values can be adjusted if the model fit to the data is not optimal. For `Hobbit_1-1T` they are taken to be 1.3 and 1.4, and for `Hobbit_MH2T`, 1.265 and 1.275, respectively.

`l` is the thickness of the sample in centimeters. For `Hobbit_1-1T` it is 3.5 cm, for `Hobbit_MH2T` it is 5.35 cm

`U_0` is the uranium concentration at the surface in ppm. This value does not significantly affect the model results and values from analyses near either surface of the sample can be used as a guide. For `Hobbit_1-1T` it is taken to be 15 ppm; for `Hobbit_MH2T`, 25 ppm.

`K_min` and `K_max` are the minimum and maximum values allowed for the uranium diffusion coefficient (in cm^2/s). Values between 10^{-13} and 10^{-11} cm^2/s are generally appropriate.

`T_min` and `T_max` are the minimum and maximum values for the age of the specimen (yr). If there is no estimated knowledge of the sample age, the range of values can be 1,000 to 500,000 yr and adjusted later. For `Hobbit_1-1T`, in the final model run, they are taken to be 50,000 and 100,000 yr, and for `Hobbit_MH2T`, 1,000 and 20,000 yr, respectively.

After setting the `U480` maximum and minimum values, run the function and adjust these min and max values by looking at the calculated `U48_0_final`, `K_final`, and `T_final`. Adjust `T_min` and `T_max` using first estimates of the age. As you iterate, increase the `nbit` value to reduce the error.

How to run the model

To run the function, attach the package and then run `iDADwig1()`, specifying the input data frame and the input parameters as described above. The code block below shows a quick example that will execute in less

117 than five seconds on a typical 2.3 GHz Intel Core i5 laptop:

```
output <- iDADwigl(Hobbit_MH2T_for_iDAD,
                  nbit = 1000,
                  fsum_target = 0.01,
                  U48_0_min = 1.265,
                  U48_0_max = 1.275,
                  l = 5.35,
                  U_0 = 25,
                  K_min = 1e-13,
                  K_max = 1e-11,
                  T_min = 1e3,
                  T_max = 20e3)
```

118 When run on the R console, this function will print a confirmation that the input data frame has the required
119 columns, and print the resulting age value with an error reported as the 67% and 33% quantiles, as follows:

```
120 All required columns are present in the input data
121 [1] "Age: 7 +0.6/-0.7 ka"
```

122 In a typical analysis we will explore the model fit by changing the range of allowed values for the ($^{234}\text{U}/^{238}\text{U}$)
123 ratio at the surface and the age of the sample, and by decreasing the `fsum_target`. Once we obtain
124 a satisfying fit (by visual inspection of the produced figures), we would increase `nbit` to a higher value
125 (e.g. 1000) and run the model again.

126 Inspecting the model's output

127 The model computes a Monte Carlo simulation where age of the sample, U diffusion coefficient and
128 ($^{234}\text{U}/^{238}\text{U}$) ratio at the surface of the sample are taken randomly within the range of values allowed.
129 Results are only kept if the calculated sum of the squared differences between the calculated and observed
130 activity ratios is less than the value set in `fsum_target`. If this is the case, the calculated ratios and the set
131 of solutions for age of the sample, U diffusion coefficient and ($^{234}\text{U}/^{238}\text{U}$) ratio at the surface of the sample
132 are saved. The model stops once the number of sets of solutions reaches `nbit`.

133 The final calculated age `T_final` (in yr), U diffusion coefficient `K_final` (in cm^2/s) and ($^{234}\text{U}/^{238}\text{U}$) ratio
134 at the surface of the sample `U48_0_final` are the set of solutions where the solution age is the closest to
135 the median age of the population of solutions. The uncertainty on each output parameter is calculated as the
136 67% and 33% quantiles of the population of solution sets.

137 T_final, K_final and U48_0_final are included in the model's output, along with their uncertainties. The
 138 function also includes a one-row data frame summarising the age:

Table 2 Summary table of the computed age and error values

| Age (ka) | Age 67% quantile (ka) | Age 33% quantile (ka) | U234_ U238_0 | U234_ U238_0 67% quantile | U234_ U238_0 33% quantile |
|----------|-----------------------|-----------------------|--------------|---------------------------|---------------------------|
| 7.016351 | 0.591806 | 0.649064 | 1.268382 | 0.006618 | 0.003382 |

139 The last item in the output is a copy of the input data with two additional columns, the calculated activity
 140 ratios, ($^{234}\text{U}/^{238}\text{U}$) and ($^{230}\text{Th}/^{238}\text{U}$), for each measurement location on the sample.

Table 3 Output table including the input data and two new columns

| iDAD.position | U234_U238_CORR | U234_U238_CORR_Int2SE | iDAD.position.1 | Th230_U238_CORR | Th230_U238_CORR_Int2SE | U_ppm | U_ppm_Int2SE | U234_U238_CALC | Th230_U238_CALC |
|---------------|----------------|-----------------------|-----------------|-----------------|------------------------|-------|--------------|----------------|-----------------|
| -0.955882 | 1.269622 | 0.00421 | -0.9558824 | 0.0733 | 0.002260 | 12.3 | 0.615 | 1.270050 | 0.0797486 |
| -0.856811 | 1.272934 | 0.00424 | -0.8568112 | 0.0732 | 0.002380 | 12.7 | 0.635 | 1.269722 | 0.0794946 |
| -0.757740 | 1.265424 | 0.00372 | -0.7577400 | 0.0760 | 0.001770 | 12.5 | 0.625 | 1.269429 | 0.0791309 |
| -0.658669 | 1.267345 | 0.00454 | -0.6586688 | 0.0770 | 0.001930 | 14.2 | 0.710 | 1.269173 | 0.0788680 |
| -0.559598 | 1.269155 | 0.00291 | -0.5595975 | 0.0721 | 0.001880 | 19.8 | 0.990 | 1.268952 | 0.0787486 |
| -0.460526 | 1.265515 | 0.00284 | -0.4605263 | 0.0769 | 0.001670 | 18.0 | 0.900 | 1.268768 | 0.0787728 |
| -0.361455 | 1.266979 | 0.00255 | -0.3614551 | 0.0816 | 0.001690 | 20.0 | 1.000 | 1.268619 | 0.0789402 |
| -0.262384 | 1.276018 | 0.00231 | -0.2623839 | 0.0786 | 0.001260 | 27.2 | 1.360 | 1.268506 | 0.0792494 |
| -0.163313 | 1.265514 | 0.00228 | -0.1633127 | 0.0753 | 0.001240 | 26.7 | 1.335 | 1.268429 | 0.0795461 |
| -0.064200 | 1.276682 | 0.00210 | -0.0642000 | 0.0731 | 0.000983 | 0.3 | 0.015 | 1.268388 | 0.0797043 |
| 0.034800 | 1.270634 | 0.00223 | 0.0348000 | 0.0779 | 0.001520 | 33.9 | 1.695 | 1.268383 | 0.0797247 |
| 0.133901 | 1.264266 | 0.00242 | 0.1339009 | 0.0666 | 0.001380 | 37.7 | 1.885 | 1.268414 | 0.0796075 |
| 0.232972 | 1.266220 | 0.00273 | 0.2329721 | 0.0713 | 0.001380 | 30.7 | 1.535 | 1.268480 | 0.0793522 |
| 0.332043 | 1.264971 | 0.00224 | 0.3320434 | 0.0773 | 0.001850 | 25.2 | 1.260 | 1.268582 | 0.0790173 |
| 0.431115 | 1.265578 | 0.00284 | 0.4311145 | 0.0832 | 0.001470 | 28.9 | 1.445 | 1.268720 | 0.0788076 |
| 0.530186 | 1.267986 | 0.00264 | 0.5301858 | 0.0864 | 0.001620 | 29.0 | 1.450 | 1.268894 | 0.0787408 |
| 0.629257 | 1.264463 | 0.00258 | 0.6292570 | 0.0816 | 0.001620 | 27.5 | 1.375 | 1.269104 | 0.0788175 |
| 0.728328 | 1.262701 | 0.00200 | 0.7283282 | 0.0704 | 0.001320 | 30.1 | 1.505 | 1.269349 | 0.0790378 |
| 0.827399 | 1.265848 | 0.00471 | 0.8273994 | 0.0953 | 0.001750 | 19.6 | 0.980 | 1.269631 | 0.0793927 |
| 0.926471 | 1.262668 | 0.00316 | 0.9264706 | 0.0958 | 0.002320 | 14.8 | 0.740 | 1.269949 | 0.0796877 |

Visualising the model's output

`iDADwig1()` returns several figures useful for visualisation of the model results along with the data:

1. a histogram of the solution ages (Figure 2 A)
2. the U concentrations in the sample as a function of the relative distance from the center (Figure 2 B)
3. the measured (in blue) and modelled (in red) ($^{234}\text{U}/^{238}\text{U}$) activity ratios as a function of the relative distance from the center (Figure 2 C), and
4. the measured (in blue) and modelled (in red) ($^{230}\text{Th}/^{238}\text{U}$) activity ratios as a function of the relative distance from the center (Figure 2 D).

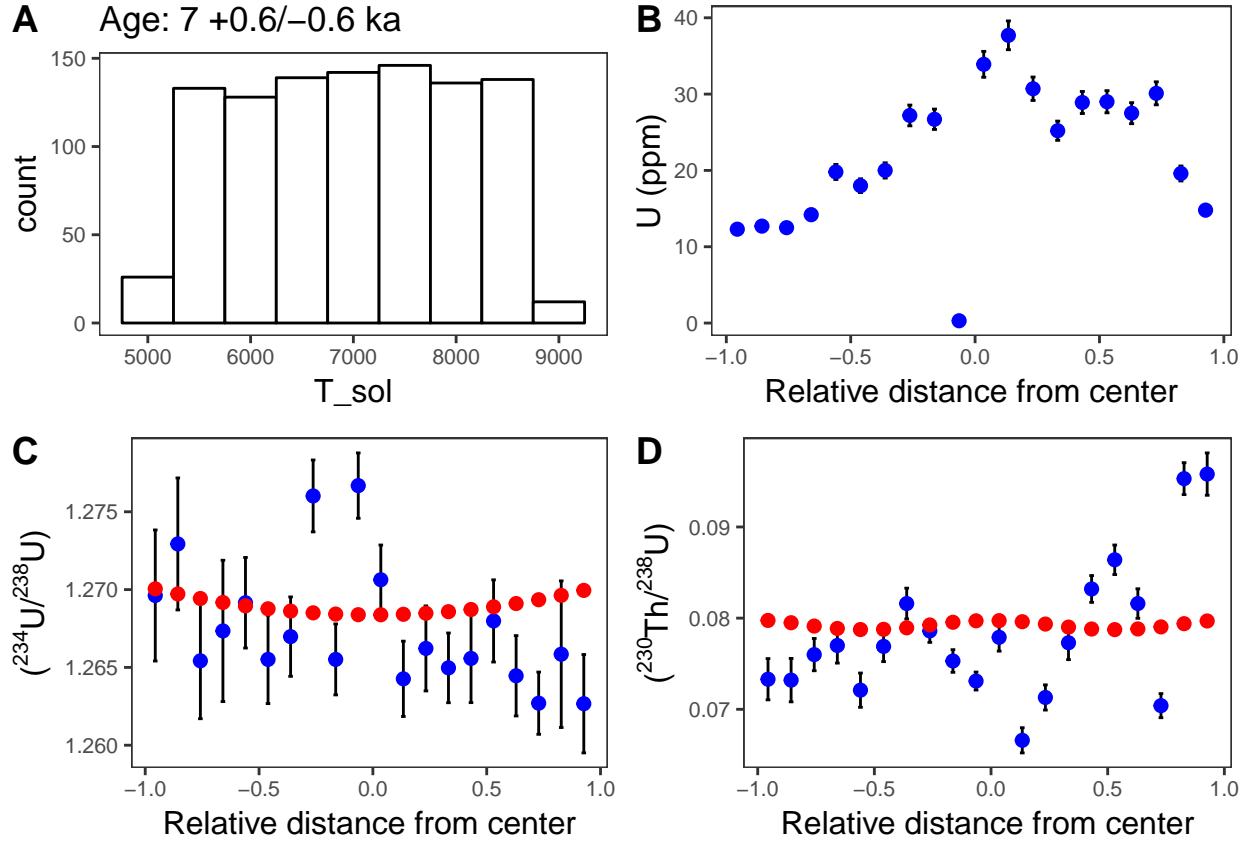


Figure 2. A: Histogram of the solution ages, B: Uranium concentration profile for transect 2 of modern human femur 132A/LB/27D/03. C: Calculated (red) and observed (blue) $(^{234}\text{U}/^{238}\text{U})$ activity ratios for transect 2 of modern human femur 132A/LB/27D/03. D: Calculated (red) and observed (blue) $(^{230}\text{Th}/^{238}\text{U})$ activity ratios for transect 2 of modern human femur 132A/LB/27D/03..

Case study of the age of the Hobbit from Sutikna et al. 2016

The package includes two sample data sets derived from Sutikna et al. (2016) : “Hobbit_MH2T_for_iDAD.csv” is data from transect 2 for modern human femur 132A/LB/27D/03. “Hobbit_1-1T_for_iDAD.csv” is data from transect 1 for *Homo floresiensis* ulna LB1/52. For the latter, six analyses were removed from the set as in Sutikna et al. (2016).

```
kableExtra::kable(Hobbit_MH2T_for_iDAD[ , 1:4],  
                  caption = "Preview of the data from transect 2 for modern human femur 132A/LB/27D/03,"  
  
kableExtra::kable(Hobbit_1_1T_for_iDAD[ , 1:4],  
                  caption = "Preview of the data from transect 1 for Homo floresiensis ulna LB1/52, inc
```

For transect 2 of 132A/LB/27D/03, Sutikna et al. (2016) reported an age of 7.4 ± 0.5 ka (thousand years before 2014). With iDADwigl, we obtain an age of $7.1 +0.6/-0.7$ ka (Figs. 2-4).

For transect 1 of LB1/52, Sutikna et al. (2016) reported an age of 79.0 ± 3.7 ka. With iDADwigl, we obtain an age of 75.4 ± 0.9 ka.

Table 4 Preview of the data from transect 2 for modern human femur 132A/LB/27D/03, included in our R package.

| iDAD.position | U234_U238_CORR | U234_U238_CORR_Int2SE | iDAD.position.1 |
|---------------|----------------|-----------------------|-----------------|
| -0.9558824 | 1.269622 | 0.00421 | -0.9558824 |
| -0.8568112 | 1.272934 | 0.00424 | -0.8568112 |
| -0.7577400 | 1.265424 | 0.00372 | -0.7577400 |
| -0.6586688 | 1.267345 | 0.00454 | -0.6586688 |
| -0.5595976 | 1.269155 | 0.00291 | -0.5595976 |
| -0.4605263 | 1.265515 | 0.00284 | -0.4605263 |
| -0.3614551 | 1.266979 | 0.00255 | -0.3614551 |
| -0.2623839 | 1.276018 | 0.00231 | -0.2623839 |
| -0.1633127 | 1.265514 | 0.00228 | -0.1633127 |
| -0.0642000 | 1.276682 | 0.00210 | -0.0642000 |
| 0.0348000 | 1.270634 | 0.00223 | 0.0348000 |
| 0.1339009 | 1.264266 | 0.00242 | 0.1339009 |
| 0.2329721 | 1.266220 | 0.00273 | 0.2329721 |
| 0.3320434 | 1.264971 | 0.00224 | 0.3320434 |
| 0.4311146 | 1.265578 | 0.00284 | 0.4311146 |
| 0.5301858 | 1.267986 | 0.00264 | 0.5301858 |
| 0.6292570 | 1.264463 | 0.00258 | 0.6292570 |
| 0.7283282 | 1.262701 | 0.00200 | 0.7283282 |
| 0.8273994 | 1.265848 | 0.00471 | 0.8273994 |
| 0.9264706 | 1.262668 | 0.00316 | 0.9264706 |

Table 5 Preview of the data from transect 1 for Homo floresiensis ulna LB1/52, included in our R package.

| iDAD.position | U234_U238_CORR | U234_U238_CORR_Int2SE | iDAD.position.1 |
|---------------|----------------|-----------------------|-----------------|
| -0.1425926 | 1.368887 | 0.00244 | -0.1425926 |
| 0.1648148 | 1.370083 | 0.00236 | 0.1648148 |
| 0.3185185 | 1.363741 | 0.00215 | 0.3185185 |
| 0.4722222 | 1.362125 | 0.00252 | 0.4722222 |
| 0.6259259 | 1.365091 | 0.00292 | 0.6259259 |
| 0.7796296 | 1.373882 | 0.00273 | 0.7796296 |

References

- Camerer C. F., Dreber A., Forsell E., Ho T.-H., Huber J., Johannesson M., Kirchler M., Almenberg J., Altmejd A., Chan T., Heikensten E., Holzmeister F., Imai T., Isaksson S., Nave G., Pfeiffer T., Razen M. and Wu H. (2016) Evaluating replicability of laboratory experiments in economics. *Science* **351**, 1433–1436. Available at: <http://science.sciencemag.org/content/351/6280/1433>.
- Camerer C. F., Dreber A., Holzmeister F., Ho T.-H., Huber J., Johannesson M., Kirchler M., Nave G., Nosek B. A., Pfeiffer T. and others (2018) Evaluating the replicability of social science experiments in nature and science between 2010 and 2015. *Nature Human Behaviour* **2**, 637.
- Collaboration O. S. and others (2015) Estimating the reproducibility of psychological science. *Science* **349**,

aac4716.

Dirks P. H., Roberts E. M., Hilbert-Wolf H., Kramers J. D., Hawks J., Dosseto A., Duval M., Elliott M., Evans M., Grun R., Hellstrom J., Herries A. I., Joannes-Boyau R., Makhubela T. V., Placzek C. J., Robbins J., Spandler C., Wiersma J., Woodhead J. and Berger L. R. (2017) The age of homo naledi and associated sediments in the rising star cave, south africa. *Elife* **6**. Available at: <https://www.ncbi.nlm.nih.gov/pubmed/28483040>.

Eggins S. M., Grün R., McCulloch M. T., Pike A. W. G., Chappell J., Kinsley L., Mortimer G., Shelley M., Murray-Wallace C. V., Spötl C. and Taylor L. (2005) In situ u-series dating by laser-ablation multi-collector icpms: New prospects for quaternary geochronology. *Quaternary Science Reviews* **24**, 2523–2538.

Freedman L. P., Cockburn I. M. and Simcoe T. S. (2015) The economics of reproducibility in preclinical research. *PLoS biology* **13**, e1002165.

Gil Y., David C. H., Demir I., Essawy B. T., Fulweiler R. W., Goodall J. L., Karlstrom L., Lee H., Mills H. J., Oh J.-H. and al. (2016) Toward the geoscience paper of the future: Best practices for documenting and sharing research from data to software to provenance. *Earth and Space Science* **3**, 388–415.

Grün R., Eggins S., Kinsley L., Moseley H. and Sambridge M. (2014) Laser ablation u-series analysis of fossil bones and teeth. *Palaeogeography, Palaeoclimatology, Palaeoecology* **416**, 150–167. Available at: <http://www.sciencedirect.com/science/article/pii/S0031018214003782>.

Hutton C., Wagener T., Freer J., Han D., Duffy C. and Arheimer B. (2016) Most computational hydrology is not reproducible, so is it really science? *Water Resources Research* **52**, 7548–7555.

Institute G. B. S. (2013) The case for standards in life science research: Seizing opportunities at a time of critical need.

Ioannidis J. P. (2005) Why most published research findings are false. *PLoS medicine* **2**, e124.

Kattge J., Díaz S. and Wirth C. (2014) Of carrots and sticks. *Nature Geoscience* **7**, 778.

Ma X. (2018) Data science for geoscience: Leveraging mathematical geosciences with semantics and open data. In *Handbook of mathematical geosciences* Springer. pp. 687–702.

Medical Sciences A. of (2015) Reproducibility and reliability of biomedical research: Improving research practice. In *Symposium report*

Miguel E., Camerer C., Casey K., Cohen J., Esterling K. M., Gerber A., Glennerster R., Green D. P., Humphreys M., Imbens G. and others (2014) Promoting transparency in social science research. *Science* **343**, 30–31.

Nosek B. A., Alter G., Banks G. C., Borsboom D., Bowman S. D., Breckler S. J., Buck S., Chambers C. D., Chin G., Christensen G. and others (2015) Promoting an open research culture. *Science* **348**, 1422–1425.

Pebesma E., Nüst D. and Bivand R. (2012) The r software environment in reproducible geoscientific research. *Eos, Transactions American Geophysical Union* **93**, 163–163.

Sambridge M., Grün R. and Eggins S. (2012) U-series dating of bone in an open system: The diffusion-adsorption-decay model. *Quaternary Geochronology*. Available at: <http://www.scopus.com/inward/record.url?eid=2-s2.0-84857958926&partnerID=40&md5=01e7f1b7d3554da26b247125425ff496>.

Sutikna T., Tocheri M. W., Morwood M. J., Saptomo E. W., Jatmiko, Awe R. D., Wasisto S., Westaway K. E., Aubert M., Li B., Zhao J.-x., Storey M., Alloway B. V., Morley M. W., Meijer H. J. M., Bergh G. D. van den, Grün R., Dosseto A., Brumm A., Jungers W. L. and Roberts R. G. (2016) Revised stratigraphy and chronology for homo floresiensis at liang bua in indonesia. *Nature* **532**, 366–369. Available at: <http://dx.doi.org/10.1038/nature17179>.

Wickham H. and Bryan J. (2018) *Readxl: Read excel files.*, Available at: <https://CRAN.R-project.org/package=readxl>.